Biophysical Chemistry 144 (2009) 78–87

Contents lists available at ScienceDirect

Biophysical Chemistry

journal homepage: http://www.elsevier.com/locate/biophyschem

Effect of curcumin on the amyloid fibrillogenesis of hen egg-white lysozyme

Steven S.-S. Wang *, Kuan-Nan Liu, Wen-Hsuan Lee

Department of Chemical Engineering, National Taiwan University, No. 1, Sec. 4, Roosevelt Road, Taipei 10617, Taiwan

ARTICLE INFO

Article history:
Received 12 February 2009
Received in revised form 25 June 2009
Accepted 27 June 2009
Available online 4 July 2009

Keywords:
Lysozyme
Amyloid fibril
Curcumin
Amyloidosis
Inhibitor

ABSTRACT

At least twenty human proteins can fold abnormally to form pathological deposits that are associated with several degenerative diseases. Despite extensive investigation on amyloid fibrillogenesis, its detailed molecular mechanisms remain unknown. This study is aimed at exploring the inhibitory activity of curcumin against the fibrillation of hen lysozyme. We found that the formation of amyloid fibrils at pH 2.0 in vitro was inhibited by curcumin in a dose-dependent manner. Moreover, quenching analysis confirmed the existence of an interaction between curcumin and lysozyme, and Van't Hoff analysis indicated that the curcumin–lysozyme interaction is predominantly governed by Van Der Waals force or hydrogen bonding. Curcumin was also found to acquire disaggregating ability on preformed lysozyme fibrils. Finally, we observed that curcumin pre-incubated at 25 °C for at least 7 days inhibited lysozyme fibrillogenesis better than untreated curcumin and the enhanced inhibition against HEWL fibrillation might be attributed to the presence of dimeric species.

© 2009 Elsevier B.V. All rights reserved.

1. Introduction

More than twenty different human peptides/proteins have been identified to fold abnormally to form pathological amyloid deposits/aggregates that have been implicated in various degenerative disorders called amyloidoses. While these unrelated amyloidogenic proteins demonstrate no sequence homology, all of them possess several common features: a β-sheet rich secondary structure, fibrillar morphology, and birefringence upon staining with Congo red [1–4]. Furthermore, accumulating evidence has revealed that proteins unrelated to amyloid diseases can aggregate in vitro to form amyloid fibrils [1,5–7]. The concept that amyloidogenicity is a general property of proteins has received renewed attention [1,8,9].

While amyloid-related diseases are at the center of intense research efforts, no real cure is currently being directed toward treating the diseases. Inhibition of the formation of fibrillar conformers and the capture of these species are viewed as effective approaches to tackling amyloidoses. Considerable efforts have been devoted to developing anti-aggregating or anti-amyloidogenic agents as potential strategies to battle amyloidoses [10,11]. Previous reports demonstrating that curcumin inhibits the aggregation of β-amyloid and α-synuclein [12–14] prompted us to further explore its influence on the fibrillation of other proteins; for example, hen egg-white lysozyme (HEWL).

HEWL, which can lyse the cell walls of bacteria, is a well-studied protein. Its monomeric form has four disulfide bonds and adopts a helix rich conformation [15]. HEWL retains a structure highly homologous to human lysozyme, which is responsible for the formation of systemic amyloidosis in the human body [16,17].

In this study, we attempted to investigate the influence of curcumin on the in vitro fibrillation of HEWL. Our results indicated that the anti-amyloidogenic activity against lysozyme fibrillation exerted by curcumin is dependent on its concentration. As evidenced by Van't Hoff analysis, a Van der Waals and/or hydrogen bonding effect was found to likely govern curcumin–HEWL interactions [18]. In addition, we observed that curcumin can disaggregate existing HEWL fibrils. Interestingly, curcumin that is pre-incubated at 25 °C for 1 week exhibits better inhibitory activity towards lysozyme aggregation as compared to untreated curcumin. This superior inhibitory potency of pre-incubated curcumin was highly associated with curcumin dimeric species formed during the course of its pre-incubation. Our data may contribute to the development of effective therapeutics for amyloidogenic diseases.

2. Experimental

2.1. Proteins and reagents

HEWL (EC 3.2.1.17) and di-sodium hydrogen phosphate were obtained from Merck (Germany). Hydrochloric acid, potassium dihydrogen phosphate, sodium chloride, and potassium chloride were purchased from Nacalai Tesque, Inc (Japan). All other chemicals, unless otherwise specified, were purchased from Sigma (USA).

2.2. Lysozyme sample preparation

HEWL sample solutions of 0.5 mg/mL were prepared in hydrochloric acid (pH 2.0) with 136.7 mM NaCl, 2.68 mM KCl and 0.01%

* Corresponding author. Tel.: +886 2 3366 5870; fax: +886 2 2362 3040.
E-mail address: sswang@ntu.edu.tw (S.S.-S. Wang).

0301-4622/$ – see front matter © 2009 Elsevier B.V. All rights reserved.
doi:10.1016/j.bpc.2009.06.010

(w/v) NaN_3. To produce the amyloid structure, HEWL solutions were incubated in a reciprocating shaker bath with a rotation rate of 30 rpm at 55 °C during the course of aggregation. Due to its light-sensitive nature, curcumin-containing HEWL samples were placed in the dark to protect them from light exposure.

2.3. Thioflavin T fluorescence (ThT) assay

Phosphate buffered saline (136.7 mM NaCl, 2.68 mM KCl, 0.01 M Na_2HPO_4, 1.76 mM KH_2PO_4, and 1.54 mM NaN_3, pH 7.4) was used to dissolve ThT to a final concentration of 10 μM. Lysozyme samples taken at different times were diluted 25-fold with ThT solution. ThT fluorescence measurements were conducted by exciting samples at 440 nm and recording the emission intensities at 490 nm averaged over 60 s on an F-2500 fluorescence spectrophotometer (Hitachi, Japan). The data were fit to the following equation [19]:

$$F = F_i + m_i t + \frac{F_f + m_f t}{1 + e^{-[(t-t_o)/\tau]}} \quad (1)$$

where F is the fluorescence intensity at time t, and t_o is the time to reach 50% of maximal fluorescence. $(F_i + m_i t)$ and $(F_f + m_f t)$ represent the initial base line corresponding to the induction period and final plateau line, respectively. The apparent rate constant for fibril growth is given by $1/\tau$, and the lag time is determined by $t_o - 2\tau$.

2.4. Intrinsic fluorescence

Steady state intrinsic fluorescence spectrum were monitored with a Cary Eclipse Fluorescence Spectrophotometer (Varian, USA) using a quartz cuvette with a path length of 0.1 cm. The measurements were recorded between 300 and 400 nm by exciting the samples at 280 nm. 40 μL of 0.5 mg/mL lysozyme samples with various concentration of curcumin were mixed with 960 μL of hydrochloric acid.

2.5. 1-Anilinonaphthalene-8-sulfonic (ANS) acid binding assay

100 μL of lysozyme samples were mixed with 900 μL of 20 μM ANS in PBS and incubated in the dark for 30 min at room temperature. ANS fluorescence intensities of mixtures taken at different times were measured by exciting the samples at 380 nm and recording the emission intensities between 420 nm and 580 nm using an F-2500 Fluorescence Spectrophotometer (Hitachi, Japan). ANS fluorescence intensity was taken at the average emission wavelength (AEW), which accounts for both changes in intensity and spectrum envelope. The determination of AEW was carried out using the following equation:

$$\mathrm{AEW} = (\Sigma F_i \lambda_i) / (\Sigma F_i) \quad (2)$$

where F_i is the ANS fluorescence intensity at wavelength λ_i.

2.6. Fluorescence quenching experiment

The lysozyme concentration of the lysozyme–curcumin mixture was 35 μM, while the concentration of curcumin was varied from 0 to 50 μM. The pH of the mixture was 2.0 and the mixture was kept at a constant temperature ranging from 10 to 55 °C. The fluorescence quenching spectra of the lysozyme–curcumin mixture were collected by exciting samples at 280 nm and recording emission intensities from 300 to 450 nm using a Cary Eclipse Fluorescence Spectrophotometer (Varian, USA). Fluorescence quenching data were analyzed according to the Lehrer equation [20]:

$$K[\mathrm{Cur}] = \frac{\beta}{1-\beta},\ \beta = \frac{F_0 - F_{\mathrm{L\cdot Cur}}}{F_0 - F_{\max}} \quad (3)$$

where K denotes the binding constant, [Cur] is the concentration of quenching agent or quencher (curcumin), and F_0 and $F_{\mathrm{L\cdot Cur}}$ are the fluorescence intensities without and with curcumin, respectively.

2.7. Transmission electron microscopy

A 10 μL sample was placed on a carbon-stabilized, formvar-coated grid. Grids were negatively stained with 2% (w/v) aqueous uranyl acetate and then examined and photographed in a JEOL, JEM-1230EX II transmission electron microscope with a Gantan Dual Vision CCD Camera (Tokyo, Japan) at an accelerating voltage of 100 kV.

3. Results

3.1. Influence of curcumin on the kinetics of HEWL fibril formation

ThT has a low fluorescence quantum yield in solution which increases considerably when bound to amyloid fibrils, displaying its high propensity to interact with amyloid fibrils [21]. As illustrated in Fig. 1A, a marked increase in the ThT fluorescence emission was observed after approximately 2–3 days of incubation with HEWL alone in hydrochloric acid (pH 2.0) with agitation at 30 rpm.

To explore if curcumin exerts inhibitory activity against the formation of HEWL fibrils at pH 2.0, we monitored the changes in ThT fluorescence intensity at various concentrations of curcumin as a function of time (shown in Fig. 1A). Also, the plateau value of emitted ThT fluorescence intensity was plotted against the concentration of curcumin and depicted in Fig. 1B. As demonstrated in Fig. 1A, approximately 3 days after the onset of incubation at 55 °C, co-incubation of HEWL with curcumin at 1, 2, 3, 5, 7, 10, 25, 50, or 100 μM was accompanied by ~3.5 ± 3.8%, ~4.4 ± 6.8%, ~11.7 ± 5.1%, ~34.3 ± 5.3%, ~41.7 ± 4.5%, ~57.2 ± 2.8%, ~73.4 ± 1.8%, ~81.5 ± 0.7%, or ~87.7 ± 0.8% reduction in the ThT fluorescence emission, respectively (the percentage reduction in ThT fluorescence intensity = 100% × (ThT fluorescence intensity of HEWL by itself − ThT fluorescence intensity of curcumin-containing HEWL sample) / ThT fluorescence intensity of HEWL by itself). The ThT fluorescence signal dropped as the curcumin concentration was increased from 1 μM to 100 μM. Among the curcumin concentrations tested, a marked reductions (>80% reduction) in ThT fluorescence emission was achieved at concentration of curcumin higher than 50 μM and almost no change in ThT fluorescence intensity was observed when the concentration of added curcumin was lower than 2 μM even after 6 days of incubation (see Fig. 1B).

The ThT fluorescence data of amyloid fibrillation exhibits a sigmoidal time-course response that can be analyzed by the nucleation-based polymerization model (the fitting equation is described in the Experimental section) [22–24]. The nucleation-dependent polymerization model could be sufficiently characterized by two parameters: the lag time of nucleation phase and the growth rate of elongation phase [19,25]. The lag time and the apparent rate constant of fibril growth for HEWL at 55 °C alone were determined to be 2.42 days and 29.09 days^{-1}, respectively. However, the presence of curcumin resulted in ~80–90% decrease in growth rate and a shorter lag time prior to rapid fibril formation.

3.2. Influence of curcumin on HEWL structure

In exploring the effect of curcumin on tertiary structure changes in HEWL, we analyzed ANS fluorescence emitted at the average emission wavelength upon excitation at 380 nm, at various incubation times. The fluorescent hydrophobic dye ANS is commonly utilized to demonstrate the presence of partially folded conformations of globular proteins and probe for conformational properties and solvent exposure of the hydrophobic surfaces in proteins [26–28]. The preferential binding of ANS to hydrophobic clusters gives rise to an

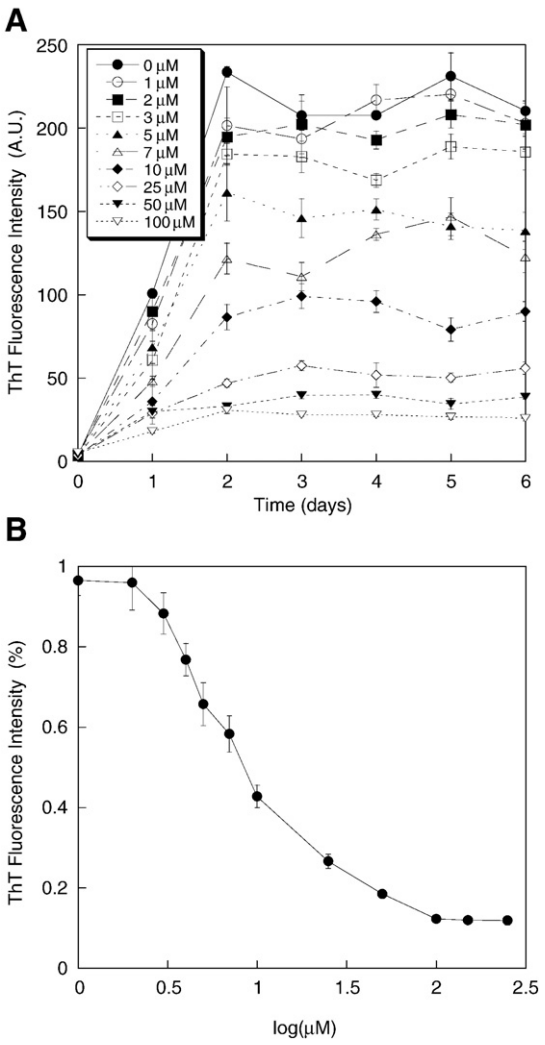

Fig. 1. The effect of curcumin on the kinetics of amyloid fibril formation of HEWL. (A) The extent of fibril formation was monitored via ThT fluorescence as a function of incubation time of the fibril formation process. The concentrations of curcumin used were 0 μM (filled circle), 1 μM (open circle), 2 μM (filled square), 3 μM (open square), 5 μM (filled upward triangle), 7 μM (open upward triangle), 10 μM (filled diamond), 25 μM (open diamond), 50 μM (filled downward triangle) and 100 μM (open downward triangle). (B) The dose–response curve plotting the plateau value of ThT fluorescence intensity of HEWL sample against the curcumin concentration. HEWL at 35 μM were dissolved in hydrochloric acid (pH 2.0) with salt and amyloid fibril formation process was performed at 55 °C. Each point represents the average of at least 5 independent measurements ($n \geq 5$).

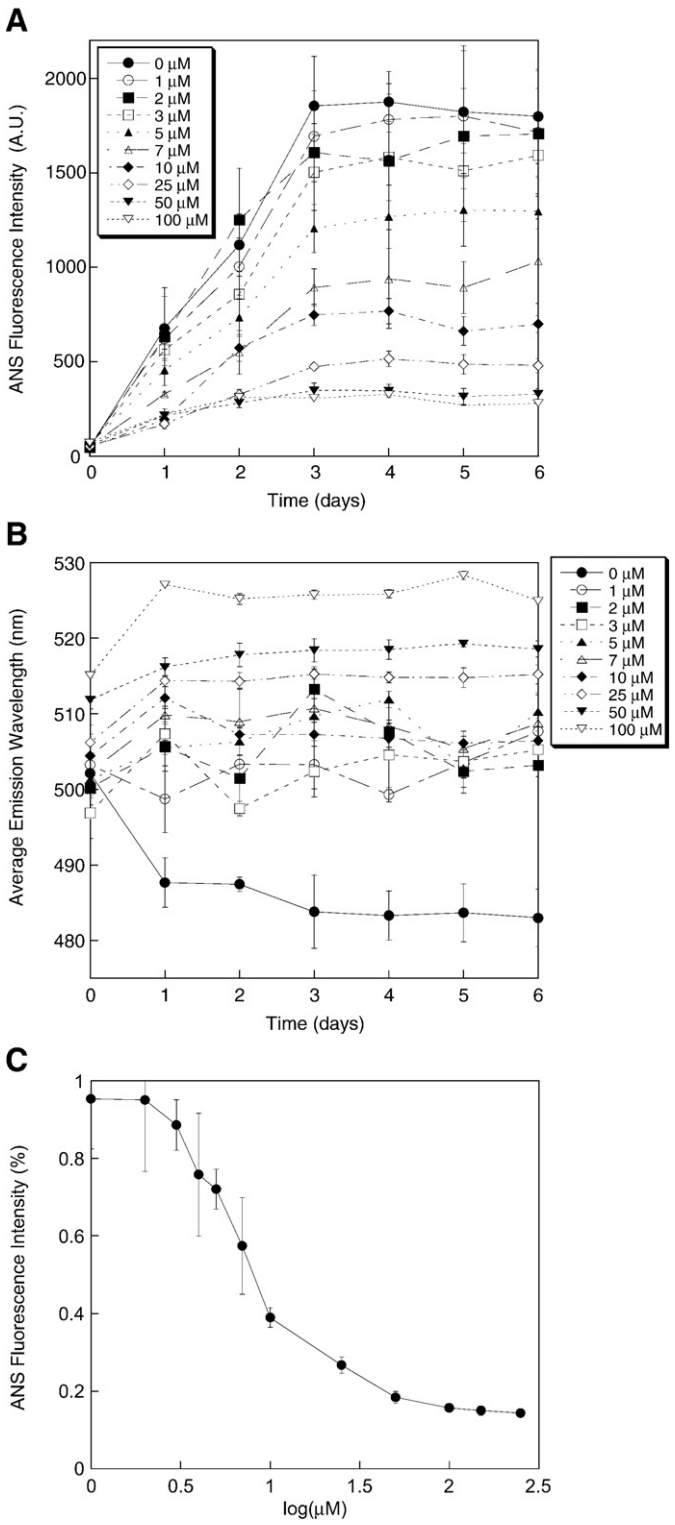

Fig. 2. The effect of curcumin on the hydrophobicity of HEWL fibrillation. The time evolution of the hydrophobicity of HEWL was measured by (A) ANS-binding fluorescence at different incubation times, (B) average emission wavelength at different incubation times. ANS fluorescence intensity was taken at the average emission wavelength. The concentrations of curcumin used were 0 μM (filled circle), 1 μM (open circle), 2 μM (filled square), 3 μM (open square), 5 μM (filled upward triangle), 7 μM (open upward triangle), 10 μM (filled diamond), 25 μM (open diamond), 50 μM (filled downward triangle) and 100 μM (open downward triangle). (C) The plateau value of ANS fluorescence intensity of HEWL sample versus the curcumin concentration. HEWL samples (35 μM) were prepared in hydrochloric acid (pH 2.0) with salt and amyloid fibril formation process was performed at 55 °C. Each point represents the average of at least 5 independent measurements ($n \geq 5$).

enhancement in fluorescence emission accompanying a blue shift of the spectral maximum [26,27,29].

We show in Fig. 2A and B that the incubation of HEWL without curcumin led to a pronounced enhancement in ANS fluorescence intensity and a drastic blue shift in the average emission wavelength (AEW), suggesting that more solvent-exposed hydrophobic regions were formed in HEWL, probably due to conformational changes in the protein leading to a partial loss of tertiary structure. However, in comparison with HEWL alone, decreasing fluorescence intensities of ANS were emitted and increasing red shifts in AEW were observed upon addition of curcumin ranging from 1 to 100 μM. This implied that the exposure of hydrophobic regions was hampered and ANS was being displaced into a more polar environment upon addition of curcumin. Moreover, the dose–response curve plotting the plateau value of the emitted ANS fluorescence intensity against the curcumin concentration was depicted in Fig. 2C.

Intrinsic fluorescence of protein, mostly owing to a highly sensitivity of fluorescence of tryptophans to their microenvironment,

has been widely employed in the research works on ligand binding, folding–unfolding, protein conformational changes [30–32]. To further understand the effect of curcumin on conformational changes in HEWL, the intrinsic fluorescence spectra of samples were also recorded. To avoid the inner filter effect [33], the samples were diluted 25-fold with hydrochloric acid before the measurement so that the absorbance of samples at the excitation wavelength 280 nm would be below 0.1. It was found that all HEWL samples (with or without curcumin) exhibited similar intrinsic fluorescence spectra before fibril formation (at $t=0$) (spectra not shown, intrinsic fluorescence intensities are shown in Fig. 3, curve 1), which ruled out the possibility of quenching due to the presence of curcumin. As depicted in Fig. 3, curve 2, a reduction in the maximum intrinsic fluorescence intensities was obtained in the fibrillar HEWL samples without curcumin (e.g., aged for 99 h), probably attributed to the quenching of solvent-exposed tryptophan residues by water during the fibril formation [32]. However, the pronounced decrease in the steady state intrinsic fluorescence intensity at the emission maximum was positively correlated with the concentration of curcumin. It was concluded from our intrinsic fluorescence and ANS fluorescence findings that more tryptophans remained buried inside and less water-exposed hydrophobic region was obtained in HEWL samples with curcumin, evidently suggesting that the conformation (or tertiary structure) of HEWL was markedly affected by the presence of curcumin.

3.3. Influence of curcumin on preformed HEWL fibrils

In order to determine the impact of curcumin on the preformed HEWL fibrils, we aggregated HEWLs under conditions analogous to those described previously for 6 days and then added curcumin at different concentrations. The effect of curcumin on existing HEWL fibrils is illustrated in Fig. 4A. The fluorescence intensities observed were not significantly different among the untreated HEWL samples for 6 days following incubation ($p>0.5$) (solid bars in Fig. 4A). However, our data showed that a substantial decline in ThT-induced fluorescence was perceived immediately upon the addition of curcumin to the sample containing preformed HEWL fibrils. For example, ~2 days after the addition of curcumin, the percentage reduction in ThT fluorescence by curcumin at 10, 25, 50, or 100 μM was approximately $77\pm3.9\%$, $88\pm0.7\%$, $93\pm0.2\%$, or $92\pm1.6\%$, respectively. We also utilized fluorescence spectroscopy combined with ANS

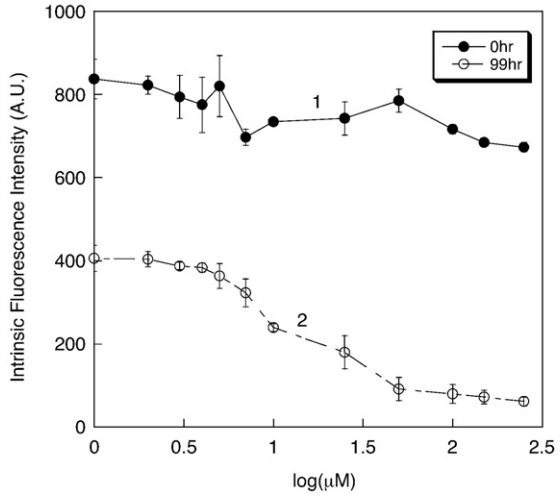

Fig. 3. Steady state fluorescence emission intensities of HEWL samples as a function of incubation time and curcumin concentration. The fluorescence emission intensities of various HEWL samples were taken at the emission wavelength of 340 nm by exciting at 280 nm. The intrinsic fluorescence intensity of HEWL sample taken at 0 h (curve 1) or 99 h (curve 2) was plotted against the curcumin concentration used.

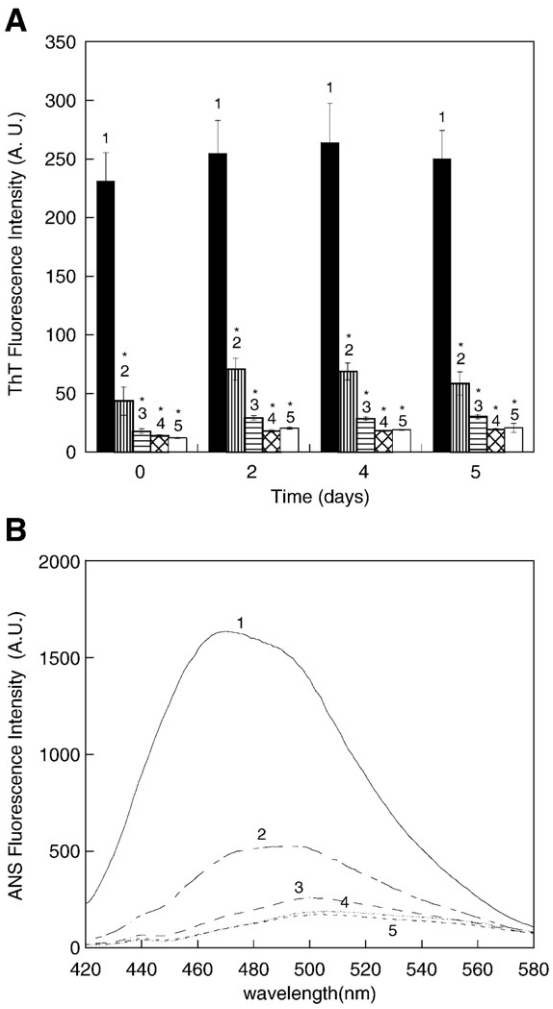

Fig. 4. The effect of curcumin on preformed HEWL fibrils. (A) ThT fluorescence emissions of 6-day preformed lysozyme fibrils in the presence of different curcumin concentrations (1: 0 μM, 2: 10 μM, 3: 25 μM, 4: 50 μM, and 5: 100 μM). Data represent the mean ThT fluorescence measurement of at least five independent experiments ($n\geq6$). Error bars represent the standard deviation (S.D.) of the ThT fluorescence measurement. *Indicates that the decrease in ThT fluorescence emission of preformed HEWL fibrils upon exposure to curcumin relative to the preformed HEWL fibrils was significant ($p<0.05$). (B) ANS fluorescence spectra of preformed lysozyme fibrils in the presence of different curcumin concentrations (curve 1: 0 μM, curve 2: 10 μM, curve 3: 25 μM, curve 4: 50 μM, and curve 5: 100 μM). HEWL (35 μM) was prepared in hydrochloric acid (pH 2.0) with salt at 55 °C and incubated for 6 days to generate preformed HEWL fibrils.

to probe for changes in surface hydrophobicity of preformed fibrils with or without curcumin. As depicted by the representative ANS fluorescence spectra in Fig. 4B, the fluorescence emission intensities were markedly attenuated and the spectra were shifted towards longer wavelengths, by at least 25 nm, upon incubation of curcumin with preformed fibrils.

3.4. Influence of curcumin on HEWL morphology

In parallel with the spectroscopic analyses, the species formed from incubation with and without curcumin were morphologically analyzed with transmission electron microscopy. Fig. 5A, B, and C show representative electron micrographs of HEWL by itself, HEWL with 50 μM curcumin, and preformed HEWL fibrils (6 days old) with subsequent addition of 50 μM curcumin, respectively. No aggregated/fibrillar species were found in fresh samples of HEWL (micrographs not shown).

Our observations confirmed that amyloid fibrils/aggregated species were formed in preformed HEWL samples (6 days after the initiation of fibrillation) in the absence of any additional molecules (see Fig. 5A). A close examination on EM micrographs revealed that preformed HEWL preparations possessed long needle-like species reminiscent of typical amyloid fibrils ~10 nm in diameter and several μm in length (with ThT fluorescence intensity of ~210.34 A.U.) (see Fig. 5A). On the contrary, as depicted in Fig. 5B, exposure of 35 μM HEWL to 50 μM curcumin resulted in a markedly reduced amount of short, sheared fibrillar species (with ThT fluorescence intensity of ~38.87 A.U.). In Fig. 5C, fewer fibrillar/aggregated species were observed in the mixture of preformed HEWL fibrils and curcumin (with ThT fluorescence intensity of ~29.49 A.U.) relative to the control sample (Fig. 5A).

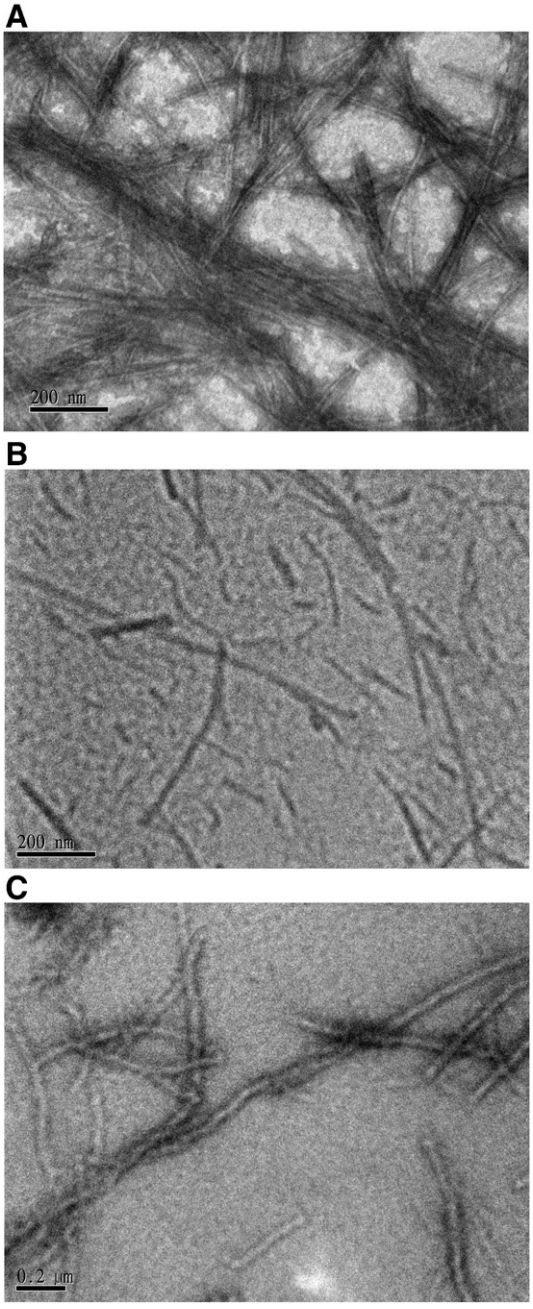

Fig. 5. Electron microscopy analysis of the anti-aggregating and disaggregating abilities of curcumin. Electron micrographs of (A) HEWL alone after 6 days of aggregation; (B) HEWL with 50 μM curcumin after 6 days of aggregation; and (C) six-day preformed HEWL fibrils incubated with 50 μM curcumin for 6 days. ThT fluorescence intensities of HEWL samples in Fig. 5A, B, and C were: ~210.34, ~38.87, and ~19.49 A.U., respectively. HEWL samples at 35 μM were prepared in hydrochloric acid (pH 2.0) with salt and the fibril formation process was conducted at 55 °C.

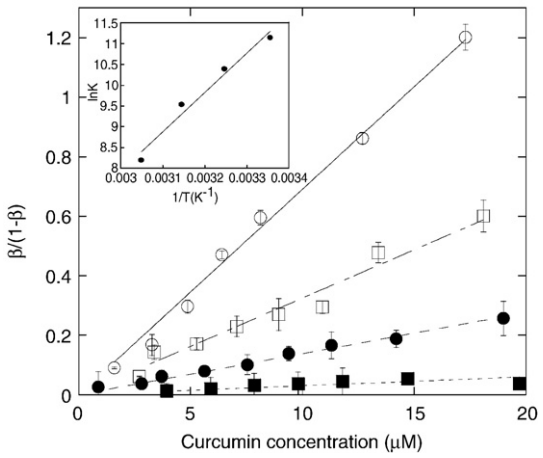

Fig. 6. Lehrer quenching plots ($\beta/(1-\beta)$) versus curcumin concentration for the HEWL–curcumin system at different temperatures (25 °C: open circle, 35 °C: open square, 45 °C: filled circle, 55 °C: filled square). Linear least-squares fitting was conducted for each straight line (line 1:25 °C, $R^2=0.997$; line 2: 35 °C, $R^2=0.991$; line 3: 45 °C, $R^2=0.997$; line 4: 55 °C, $R^2=0.997$). Data points represent the mean values obtained from at least 4 independent experiments ($n\geq 4$). The inset shows the linear plot of ln$K$ versus 1 / T. The binding constant (K) at each temperature was obtained from the slope of each corresponding straight line.

Our TEM findings allowed us to conclude that curcumin serves as a potential molecule with inhibitory and disaggregating properties against HEWL fibrillation. By combining with our ThT fluorescence results, it was found that the suppressing effect of curcumin on HEWL aggregation/fibril formation at 55 °C followed a concentration-dependent manner. In addition, IC_{50}, defined by the concentration at which half of the HEWL ThT fluorescence intensity is reduced, was used to present the effectiveness of curcumin in inhibiting HEWL fibrillation. According to an analysis of dose–dependent curve shown in Fig. 1B, IC_{50} of curcumin was determined to be ~7.7 μM.

3.5. Characteristics of Interaction between curcumin and HEWL

Fluorescence quenching is a process in which the emitted fluorescence intensity of a protein is weakened by a number of molecular interactions such as excited-state reaction, molecular rearrangement, and ground state complex formation [34–36].

We investigated the fluorescence quenching of HEWL induced by curcumin at different temperatures (10, 25, 40, and 55 °C). After plotting the fluorescence quenching spectra of HEWL with varying concentrations of curcumin, it was found that the fluorescence signal decreased regularly with an increasing concentration of curcumin. The mechanism of curcumin-induced fluorescence quenching of HEWL was identified by analyzing the fluorescence quenching data using the Lehrer equation as shown in the Experimental section. As shown in Fig. 6, at a constant temperature, perfect linearity was observed between $\beta/(1-\beta)$ and the curcumin concentration and estimates of

Table 1
A listing of binding constants and thermodynamic parameters of the interaction between hen egg-white lysozyme and curcumin.

Temperature (°C)	K (M^{-1})	ΔG (J/mol)	Van't Hoff analysis	
			ΔH (J/mol)	ΔS (J/mol K)
25	68,985	−27,606.9	−78,390.7	−169.17
35	32,467	−26,603.2		
45	13,800	−25,204.7		
55	3630	−22,355.5		

Table 2
The effects of aging duration and temperature on the inhibitory potency of curcumin against fibril formation of hen egg-white lysozymes.

	10 μM					50 μM				
	25 °C (7 d)	55 °C (7 d)	25 °C (24 d)	55 °C (24 d)	w/o	25 °C (7 d)	55 °C (7 d)	25 °C (24 d)	55 °C (24 d)	w/o
Day 2	79.83%	48.85%	68.63%	21.11%	62.96%	91.12%	77.41%	78.59%	41.77%	85.87%
Day 4	77.82%	43.37%	76.74%	35.38%	53.80%	90.35%	60.50%	85.77%	56.86%	80.68%
Day 6	73.56%	49.42%	73.40%	19.77%	57.23%	89.70%	66.61%	85.61%	57.73%	81.52%

Several pre-incubation conditions of curcumins were used before mixing with hen egg-white lysozymes: fresh or without pre-incubation (w/o), pre-incubated for 7 days at 25 °C (25 °C (7 d)), pre-incubated for 24 days at 25 °C (25 °C (24 d)), pre-incubated for 7 days at 55 °C (55 °C (7 d)), and pre-incubated for 24 days at 55 °C (55 °C (24 d)). The fibril formation of hen lysozyme with fresh or pre-incubated curcumin was carried out at pH 2.0 and 55 °C. The percentage values in the table were the percentage reductions in ThT fluorescence intensity measured relative to that of the lysozyme sample unexposed to curcumin (control) and determined by the following formula:

$$\text{Percentage reduction in ThT fluorescence intensity} = (F_0 - F)/F_0 \times 100\%$$

where F_0 and F denote ThT fluorescence intensity of HEWL by itself (0 μM curcumin) and ThT fluorescence intensity of HEWL sample with 10 or 50 μM curcumin. The inhibitory potency could be represented by the percentage reduction in ThT fluorescence intensity. A larger percentage reduction in ThT fluorescence intensity was indicative of greater efficiency or inhibitory potency of curcumin against HEWL fibrillation.

the slopes or the binding constants (K) were obtained by fitting straight lines via least-squares regressions. As listed in Table 1, it is apparent that the magnitude of the resultant binding constant is negatively correlated with incubation temperature, suggesting that curcumin-induced fluorescence quenching of HEWL is predominated by the Van der Waals force or hydrogen bonding [18,37,38].

Van't Hoff analysis of the temperature-dependent binding data was conducted to retrieve further information regarding the mode of the interaction force (see inset of Fig. 6). Thermodynamic parameters, ΔH, ΔG, and ΔS, were determined and listed in Table 1. Our data indicated that the curcumin–HEWL binding is a spontaneous ($\Delta G<0$) and exothermic ($\Delta H<0$) interaction, and the associated change in 321 entropy is negative ($\Delta S<0$).

It should be noted that, in Van't Hoff analysis, the ΔH and ΔS of the binding interaction were assumed to be approximately constant over the range of temperatures used. This is why we could only obtain one value for ΔH or ΔS.

3.6. Effect of pre-incubated curcumin on HEWL fibrillogenesis

It has been reported that the structure or distribution of curcumin varies with incubation condition (e.g., temperature, pH, or solvent type) [39–42]. As a preliminary screening, we first monitored the time evolution of UV–Vis absorption spectra of curcumin and found that distinctive UV–Vis spectra were obtained under various pre-incubation durations and temperatures (spectra not shown), suggestive of the temporal and temperature dependence of structural alteration of curcumin. Next, we wanted to test whether pre-incubation of curcumin at various temperatures could affect its inhibitory potency against HEWL fibril formation. We pre-incubated curcumin (10, 25, 50, and 100 μM) at 25 or 55 °C for various periods of time prior to initiating HEWL aggregation at 55 °C. As summarized in Table 2, when curcumin was pre-incubated at 25 °C for either 7 or 24 days, an increase in inhibitory activity against HEWL fibrillation was detected as the concentration of curcumin used was elevated from 10 to 50 μM.

If the percentage reduction in ThT fluorescence intensity measured in curcumin-containing HEWL sample relative to that of the control sample unexposed to curcumin was used to represent the inhibitory potency or inhibitory effect of curcumin against HEWL fibrillation, a greater efficiency or inhibitory potency of curcumin would be obtained in situations where more ThT fluorescence decrease was detected by the addition of inhibitor (e.g.: a larger percentage reduction in ThT fluorescence intensity). We show in Table 2 that, when pre-incubated for 7 or 24 days, 25 °C-pretreated curcumin exhibited a superior inhibitory effect on HEWL fibril formation relative to untreated curcumin. For example, approximately 6 days after the outset of the aggregation process at 55 °C, ~89.70 ± 0.5%, ~85.61 ± 1.5%, and ~81.52 ± 0.7% reductions in ThT-induced emission occurred for HEWL plus 50 μM curcumin with 7, 24 days pre-incubation at 25 °C, and fresh untreated curcumin, respectively (see Table 2). As indicated in Table 2, the percentage reduction in ThT fluorescence resulting from the addition of 50 μM curcumin pre-incubated at 55 °C for approximately 7 days (77.41 ± 3.5% (Day 2), 60.50 ± 0.9% (Day 4), 66.61 ± 1.6% (Day 6)) was lower than that obtained from HEWL solution containing 50 μM curcumin without any pre-incubation (85.87 ± 0.7% (Day 2), 80.68 ± 1.06% (Day 4), 81.52 ± 0.7% (Day 6)), implying that curcumin prepared in this specific pre-incubation condition (55 °C, ~7 days) was less potent than its fresh/untreated counterpart in inhibiting HEWL fibril formation. Furthermore, with 50 μM curcumin pre-incubated at 55 °C for up to 24 days before mixing with HEWL, a significantly lower inhibitory effect was evident relative to that of the HEWL solution containing untreated/fresh curcumin. Overall, the inhibitory potencies induced by curcumin in different pre-incubation conditions were in the following order: 7-day pre-incubation at 25 °C, 24-day pre-incubation at 25 °C > untreated > 7-day pre-incubation at 55 °C > 24-day pre-incubation at 55 °C.

Moreover, further confirmation that the inhibitory potency against HEWL fibrillation induced by 25 °C pre-incubated curcumin came from electron microscopy analysis. With co-incubation of HEWLs with 25 °C pre-incubated curcumin, fewer shorter fibrils were detected relative to those observed in samples of HEWLs with untreated curcumin (micrographs not shown).

3.7. Mass spectrometric analysis of curcumin under various pre-incubation conditions

Our preceding results revealed that curcumin pre-incubated at 25 °C for 7 days has the highest inhibitory potency against HEWL fibril formation, and this curcumin-induced inhibition is strongly dependent on its pre-incubation. Mass spectrometry using an electrospray ionization source (ESI) in the positive ionization mode with Finnegan LCQ was employed to gain further insight into the variations in structure and composition among curcumin samples with different pre-treatments. Fig. 7A, B, and C demonstrate the representative ESI positive spectra of freshly prepared 50 μM curcumin, 50 μM curcumin pre-incubated at 25 °C for 16 days, and 50 μM curcumin pre-incubated at 55 °C for 16 days, respectively. We show in Fig. 7A that, apart from the solvent peak at $m/z = 223.27$, two major peaks at $m/z = 369.33$ and $m/z = 339.40$ corresponding to curcumin and demethoxycurcumin (with one $-OCH_3$ removed from curcumin) [43], respectively, were detected in the fresh curcumin. However, the 16 days pre-incubation of curcumin at 25 °C resulted in the generation of a group of peaks at $m/z = 701.60$–761.60. After comparing our data with the one reported in previous work [79,80], the peak at $m/z = 761.60$ was identified to as molecular ion of curcumin dimer while the peaks at

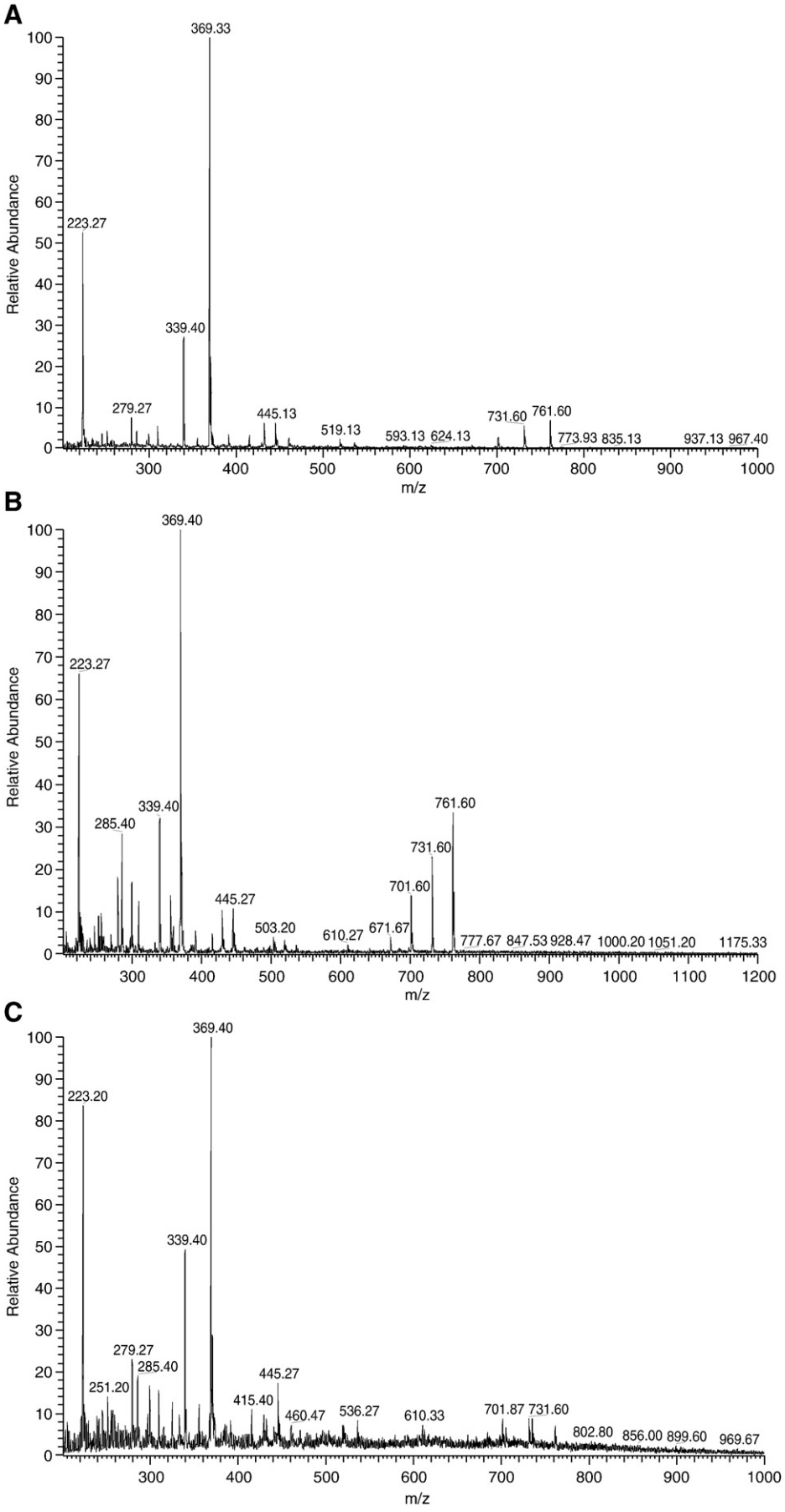
A
Relative Abundance
m/z
369.33
223.27
339.40
279.27
445.13
519.13
593.13
624.13
731.60
761.60
773.93
835.13
937.13
967.40
B
Relative Abundance
m/z
369.40
223.27
339.40
285.40
445.27
503.20
610.27
671.67
701.60
731.60
761.60
777.67
847.53
928.47
1000.20
1051.20
1175.33
C
Relative Abundance
m/z
369.40
223.20
339.40
279.27
285.40
251.20
445.27
415.40
460.47
536.27
610.33
701.87
731.60
802.80
856.00
899.60
969.67

$m/z = 731.60$ and 701.60 were resulted from the reduction of one and two $-OCH_3$ groups, respectively (see Fig. 7B). In addition, the amount of curcumin (and demethoxycurcumin) was reduced as compared with the relative abundance of solvent peak (e.g.: the ratio of curcumin to solvent was from ~100:53 to ~100:66.5). As revealed in Fig. 7C, when pre-incubated at the elevated temperature (55 °C), curcumin and demethoxycurcumin were the two most populated molecular ions, and importantly, no trace of dimer species was found in the curcumin sample.

4. Discussion

A variety of evidence suggests a strong connection between amyloid fibril formation and disease pathology. Amyloid fibrils or protofibrils derived from aggregated amyloid proteins have been demonstrated to be closely associated with *in vitro* cytotoxicity [44–46]. The toxic effects elicited by these proteins have been prevented by compounds that bind to amyloid fibrils or inhibit fibril formation [47–49]. Reducing the β-sheet content and formation of fibrils are considered two promising therapeutic approaches to limit the development of amyloidoses.

Numerous molecules have been reported to retard or inhibit the formation of amyloid fibrils both *in vitro* and *in vivo*. In general, these compounds can be divided into two groups: non-peptidic and peptidic inhibitors. Non-peptidic inhibitors, consisting of a wide range of chemical and natural compounds, include aromatic phenolic ring-bearing polyphenols (e.g., nordihydroguaiaretic acid and rosemarinic acid) [11], benzofuran-based compounds (e.g., Congo red and its napthylazo derivatives) [50,51], semisynthetic bacteriocidal antibiotic drugs (e.g., rifampicin and its derivatives) [52,53], surfactants molecules (e.g., di-C6-PC, di-C7-PC, and n-dodecylhexaoxyethylene glycol monoether) [2,54,55] and others (e.g., nicotine, melatonin, and trehalose) [10,11,56–58]. Due to their marked affinity for amyloid proteins, certain shorter peptide fragments serve as self-recognition sequences to disrupt amyloid fibril formation [59–61]. Moreover, other peptidic molecules that have been revealed to possess inhibitory effects on amyloid fibrillation or cytotoxicity fall into a category of small heat shock proteins (e.g., alpha-crystallin Hsp20) [62,63].

Curcumin, the main ingredient of turmeric and widely used for food spicing and coloring, is a low molecular-weight, naturally-occurring phytochemical that is isolated from the rhizome of the *Curcuma longa* plant. It is an important polyphenolic and the principal active ingredient in the widely used spice turmeric. Curcumin protects the brain from lipid peroxidation and serves as a free radical scavenger and an antioxidant [64–70]. In addition, curcumin has long been known to possess anti-inflammatory and anti-carcinogenic activities [71–74]. It has been suggested that the chemopreventive activity of curcumin might be attributed to its ability to induce apoptosis [75–77].

Apart from those aforementioned properties, perhaps due to its structural resemblance to a well-known amyloid specific azo-dye Congo red, curcumin has also been shown to exert anti-fibrillogenic activity or disaggregating property against the fibrillation/aggregation of various amyloid proteins such as α-synuclein of Parkinson's disease and β-amyloid peptide of AD [12–14]. In these studies, curcumin was shown to destabilize preformed fibrillar species in a concentration-dependent manner. It was also suggested that a decrease in the net extension rate of amyloid proteins may result from the binding of curcumin at the terminus of the extending amyloid protein followed by conformational stabilization [12,13]. With the aid of synthetic β-amyloid peptides and a transgenic mouse model (Tg2576), Yang and coworkers examined the impact of curcumin on amyloid accumulation *in vitro* and *in vivo* [14]. They concluded that curcumin inhibits *in vitro* β-amyloid fibril formation, blocks *in vitro* β-amyloid-induced cytotoxicity, and lowers plaque burden in transgenic mice [14]. Moreover, curcumin has been reported to attenuate oxidative damage and amyloid pathology in the brains of Alzheimer's disease-related Swedish mutant transgenic mice [78].

We first showed in our study that, in the presence of salt, rapid formation of HEWL fibrils under acidic conditions occurs (Fig. 1A). Next, curcumin was tested for its effect on *in vitro* fibrillogenesis of HEWL. We demonstrated with ThT fluorescence enhancement and transmission electron microscopy that curcumin, at a concentration range of 1–100 μM, inhibits the fibrillation of HEWL (Figs. 1 and 5). Our observations also revealed that co-incubation of HEWL with curcumin is accompanied by a reduction in ANS-induced fluorescence emission, and this reduction is positively correlated with curcumin concentration, implying that a decrease in ANS binding-competent solvent-exposed hydrophobic regions occurs with an increase in curcumin concentration (Fig. 2A, B, and C). Analogous to ANS fluorescence results, the decline of intrinsic fluorescence intensity at the emission maximum is dependent upon the curcumin concentration, illustrating that curcumin greatly affects the three-dimensional locations of tryptophan residues and the hydrophobic regions of HEWL. In addition, experiments using HEWL treated with curcumin at later times during the incubation showed that curcumin presents disaggregating activity against existing HEWL fibrils (Fig. 4A).

Fluorescence quenching spectra of samples were monitored in order to understand the type of binding force associated with the interaction between curcumin and HEWL. We found that the binding constant decreases with increasing temperature and concluded that the probable HEWL fluorescence quenching mechanism by curcumin is Van der Waals force or hydrogen bonding (Table 1, and Fig. 6). To gain insights into the nature of the curcumin–HEWL interactions, a Van't Hoff analysis of the temperature-dependent binding data was performed and our results demonstrated that the observed curcumin–protein interaction was exothermic as well as spontaneous (Table 1 and inset of Fig. 6). Also, the entropy change associated with the interaction was determined to be negative, suggesting that the favorable curcumin–HEWL interaction is enthalpy-driven and probably governed by Van der Waals force or hydrogen bonding [18].

Finally, if curcumin was allowed to incubate at 25 °C for 7 days prior to addition to the HEWL solution, a pronounced elevation in inhibitory action against HEWL fibrillation was found (Table 2). However, in comparison with the HEWL solution plus untreated curcumin, no prominent decline in ThT-induced fluorescence emission was detected when mixing HEWL with curcumin pre-incubated at 55 °C for greater than 24 days (Table 2). It could be concluded from our results that the curcumin pre-incubated for 7 or 24 days at 25 °C exhibited a superior inhibitory activity to that of the untreated curcumin or curcumin pre-incubated at 55 °C. Furthermore, results from our mass spectrometric analysis suggested that the enhanced inhibitory potency against HEWL fibrillation might be attributed to the presence of dimeric species formed in the aged curcumin solution at 25 °C. It has been documented that, due to its radical termination nature, the generation of dimeric form of curcumin has a significant contribution to the antioxidant activity of curcumin [79,80]. Moreover, others have reported that dimeric species of curcumin can selectively destroys human neurotumor cells, suggesting curcumin dimer's critical role in anti-tumor activity [81].

Several lines of evidence suggest that curcumin has an inhibitory effect on the conversion of prion protein (PrP) *in vitro* [82] and in scrapie agent-infected neuroblastoma cell line [83]. Through several spectroscopic analyses, recent research on how curcumin inhibits PrP^{Sc} aggregation has demonstrated that curcumin was able to recognize α-helix rich intermediate, β-sheet rich oligomeric, β-

Fig. 7. Mass spectra of curcumin with various pre-incubation conditions in positive ion mode. (A) fresh curcumin; (B) curcumin was pre-incubated at 25 °C for 16 days; (C) curcumin was pre-incubated at 55 °C for 16 days.

sheet rich fibrillar species, and plaques of PrP, but not its α-helix rich native conformer [84]. Additionally, the conclusion made by the authors is two-fold: (1) the intervention of α-to-β conversion of PrP could be achieved via the preferential binding of curcumin to the α-helix rich intermediate, (2) the fibrillar prion species can be captured by curcumin thus leading to the prevention of fibril growth and seed generation [84].

Polyphenols belong to a large group of natural and synthetic small molecules that are composed of one or more aromatic phenolic rings. Natural polyphenols, widely found in wine, tea, and plants, can be categorized into three groups: phenolic acids (e.g., benzoic acid), flavonoids (e.g., flavanone), and non-flavonoid polyphenols (e.g., curcumin) [11,74]. Given the fact that the aromatic residues are commonly present in amyloid-forming proteins, the role of aromatic stacking or p–p interactions has been suggested to play a major role in amyloid fibrillation [11,85,86]. With the involvement of aromatic phenolic rings, it is reasonable to suspect that curcumin may induce an inhibitory effect toward fibril formation. Further experimental or theoretical work, however, is needed to confirm this hypothesis.

In conclusion, our work revealed that curcumin can inhibit HEWL fibrillation and also induce disaggregation of existing HEWL fibrillar species. Importantly, we, for the first time, found that curcumin pre-incubated under certain conditions has improved inhibitory activity against lysozyme fibrillation as compared to fresh curcumin. This superior inhibitory potency of pre-incubated curcumin was highly associated with certain curcumin derivative, dimeric species in particular, formed during the course of its pre-incubation. While further investigations are essential to clarify the role of curcumin in inhibiting or preventing HEWL fibrillation, we believe that our results are important for the rational design of potential therapeutics for amyloidoses.

Acknowledgement

This work was supported by grants from the National Science Council, Taiwan.

References

[1] C.M. Dobson, Principles of protein folding, misfolding and aggregation, Semin. Cell Dev. Biol. 15 (2004) 3–16.
[2] S.S.S. Wang, T.A. Good, An overview of Alzheimer's disease, J. Chin. Ins. Chem. Eng. 36 (2005) 533–559.
[3] C.A. Ross, M.A. Poirier, Protein aggregation and neurodegenerative disease, Nat. Med. 10 (Suppl) (2004) S10–S17.
[4] V.N. Uversky, A.L. Fink, Conformational constraints for amyloid fibrillation: the importance of being unfolded, Biochim. Biophys. Acta 1698 (2004) 131–153.
[5] M.D. Shtilerman, T.T. Ding, P.T. Lansbury Jr., Molecular crowding accelerates fibrillization of alpha-synuclein: could an increase in the cytoplasmic protein concentration induce Parkinson's disease? Biochemistry 41 (2002) 3855–3860.
[6] E. Frare, P.P. de Laureto, J. Zurdo, C.M. Dobson, A. Fontana, A highly amyloidogenic region of hen lysozyme, J. Mol. Biol. 340 (2004) 1153–1165.
[7] S. Fujiwara, F. Matsumoto, Y. Yonezawa, Effects of salt concentration on association of the amyloid protofilaments of hen egg white lysozyme studied by time-resolved neutron scattering, J. Mol. Biol. 331 (2003) 21–28.
[8] M. Fandrich, V. Forge, K. Buder, M. Kittler, C.M. Dobson, S. Diekmann, Myoglobin forms amyloid fibrils by association of unfolded polypeptide segments, Proc. Natl. Acad. Sci. U. S. A. 100 (2003) 15463–15468.
[9] Y. Kallberg, M. Gustafsson, B. Persson, J. Thyberg, J. Johansson, Prediction of amyloid fibril-forming proteins, J. Biol. Chem. 276 (2001) 12945–12950.
[10] L.D. Estrada, C. Soto, Disrupting beta-amyloid aggregation for Alzheimer disease treatment, Curr. Top. Med. Chem. 7 (2007) 115–126.
[11] Y. Porat, A. Abramowitz, E. Gazit, Inhibition of amyloid fibril formation by polyphenols: structural similarity and aromatic interactions as a common inhibition mechanism, Chem. Biol. Drug. Des. 67 (2006) 27–37.
[12] K. Ono, K. Hasegawa, H. Naiki, M. Yamada, Curcumin has potent anti-amyloidogenic effects for Alzheimer's beta-amyloid fibrils in vitro, J. Neurosci. Res. 75 (2004) 742–750.
[13] K. Ono, M. Yamada, Antioxidant compounds have potent anti-fibrillogenic and fibril-destabilizing effects for alpha-synuclein fibrils in vitro, J. Neurochem. 97 (2006) 105–115.
[14] F. Yang, G.P. Lim, A.N. Begum, O.J. Ubeda, M.R. Simmons, S.S. Ambegaokar, P.P. Chen, R. Kayed, C.G. Glabe, S.A. Frautschy, G.M. Cole, Curcumin inhibits formation of amyloid beta oligomers and fibrils, binds plaques, and reduces amyloid in vivo, J. Biol. Chem. 280 (2005) 5892–5901.
[15] M.C. Vaney, S. Maignan, M. Ries-Kautt, A. Ducriux, High-resolution structure (1.33 A) of a HEW lysozyme tetragonal crystal grown in the APCF apparatus. Data and structural comparison with a crystal grown under microgravity from SpaceHab-01 mission, Acta Crystallogr., D Biol. Crystallogr. 52 (1996) 505–517.
[16] M.B. Pepys, P.N. Hawkins, D.R. Booth, D.M. Vigushin, G.A. Tennent, A.K. Soutar, N. Totty, O. Nguyen, C.C. Blake, C.J. Terry, et al., Human lysozyme gene mutations cause hereditary systemic amyloidosis, Nature 362 (1993) 553–557.
[17] M. Dumoulin, J.R. Kumita, C.M. Dobson, Normal and aberrant biological self-assembly: insights from studies of human lysozyme and its amyloidogenic variants, Acc. Chem. Res. 39 (2006) 603–610.
[18] P.D. Ross, S. Subramanian, Thermodynamics of protein association reactions: forces contributing to stability, Biochemistry 20 (1981) 3096–3102.
[19] L. Nielsen, R. Khurana, A. Coats, S. Frokjaer, J. Brange, S. Vyas, V.N. Uversky, A.L. Fink, Effect of environmental factors on the kinetics of insulin fibril formation: elucidation of the molecular mechanism, Biochemistry 40 (2001) 6036–6046.
[20] S.S. Lehrer, G.D. Fasman, Fluorescence of lysozyme and lysozyme substrate complexes, Biochem. Biophys. Res. Comm. 23 (1966) 133–138.
[21] H. LeVine III, Thioflavine T interaction with synthetic Alzheimer's disease beta-amyloid peptides: detection of amyloid aggregation in solution, Protein. Sci. 2 (1993) 404–410.
[22] Y.A. Berlin, A.L. Burin, L.D.A. Siebbeles, M.A. Ratner, Conformationally gated rate processes in biological macromolecules, J. Phys. Chem., A 105 (2001) 5666–5678.
[23] J. Nelson, R.E. Chandler, Random walk models of charge transfer and transport in dye sensitized systems, Coord. Chem. Rev. 248 (2004) 1181–1194.
[24] M. Kodaka, Requirements for generating sigmoidal time-course aggregation in nucleation-dependent polymerization model, Biophys. Chemist. 107 (2004) 243–253.
[25] J.D. Harper, P.T. Lansbury Jr., Models of amyloid seeding in Alzheimer's disease and scrapie: mechanistic truths and physiological consequences of the time-dependent solubility of amyloid proteins, Annu. Rev. Biochem. 66 (1997) 385–407.
[26] C.P. Liu, Z.Y. Li, G.C. Huang, S. Perrett, J.M. Zhou, Two distinct intermediates of trigger factor are populated during guanidine denaturation, Biochimie 87 (2005) 1023–1031.
[27] A.L. Smoot, M. Panda, B.T. Brazil, A.M. Buckle, A.R. Fersht, P.M. Horowitz, The binding of bis-ANS to the isolated GroEL apical domain fragment induces the formation of a folding intermediate with increased hydrophobic surface not observed in tetradecameric GroEL, Biochemistry 40 (2001) 4484–4492.
[28] I. Sirangelo, E. Bismuto, S. Tavassi, G. Irace, Apomyoglobin folding intermediates characterized by the hydrophobic fluorescent probe 8-anilino-1-naphthalene sulfonate, Biochim. Biophys. Acta 1385 (1998) 69–77.
[29] G.V. Semisotnov, N.A. Rodionova, O.I. Razgulyaev, V.N. Uversky, A.F. Gripas, R.I. Gilmanshin, Study of the "molten globule" intermediate state in protein folding by a hydrophobic fluorescent probe, Biopolymers 31 (1991) 119–128.
[30] M.R. Eftink, Fluorescence techniques for studying protein-structure, Methods Biochem. Anal. 35 (1991) 127–205.
[31] M.R. Eftink, The use of fluorescence methods to monitor unfolding transitions in proteins, Biochem.-Moscow 63 (1998) 276–284.
[32] E. Di Stasio, P. Bizzarri, F. Misiti, E. Pavoni, A. Brancaccio, A fast and accurate procedure to collect and analyze unfolding fluorescence signal: the case of dystroglycan domains, Biophys. Chemist. 107 (2004) 197–211.
[33] L. Brand, B. Witholt, C.H.W. Hirs, [87] Fluorescence measurements, Methods in Enzymology, Academic Press, 1967, pp. 776–856.
[34] Y.J. Hu, Y. Liu, W. Jiang, R.M. Zhao, S.S. Qu, Fluorometric investigation of the interaction of bovine serum albumin with surfactants and 6-mercaptopurine, J. Photochem. Photobiol., B 80 (2005) 235–242.
[35] A.Q. Gong, X.S. Zhu, Y.Y. Hu, S.H. Yu, A fluorescence spectroscopic study of the interaction between episteride and bovin serum albumine and its analytical application, Talanta 73 (2007) 668–673.
[36] J.F. Zhu, X. Zhang, D.J. Li, J. Jin, Probing the binding of flavonoids to catalase by molecular spectroscopy, J. Mol. Struct. 843 (2007) 38–44.
[37] K. Katsumata, A. Okazaki, G.P. Tsurupa, K. Kuwajima, Dominant forces in the recognition of a transient folding intermediate of alpha-lactalbumin by GroEL, J. Mol. Biol. 264 (1996) 643–649.
[38] H. Kondo, M. Shiroishi, M. Matsushima, K. Tsumoto, I. Kumagai, Crystal Structure of anti-hen egg white lysozyme antibody (HyHEL-10) Fv–antigen complex. Local structural changes in the protein antigen and water-mediated interactions of Fv–antigen and light chain–heavy chain interfaces, J. Biol. Chem. 274 (1999) 27623–27631.
[39] B.T. Kurien, A. Singh, H. Matsumoto, R.H. Scofield, Improving the solubility and pharmacological efficacy of curcumin by heat treatment. Assay and drug development, Technologies 5 (2007) 567–576.
[40] S.M.S. Chauhan, A.S. Kandadai, N. Jain, A. Kumar, Biomimetic oxidation of curcumin with hydrogen peroxide catalyzed by 5,10,15,20-tetraarylporphyrinatoiron(III) chlorides in dichloromethane, Chem. Pharm. Bull.. 51 (2003) 1345–1347.
[41] G. Jones, W.R. Jackson, C. Choi, W.R. Bergmark, Solvent effects on emission yield and lifetime for coumarin laser-dyes — requirements for a rotatory decay mechanism, J. Phys. Chem. 89 (1985) 294–300.
[42] K. Ohara, W. Mizukami, A. Tokunaga, S.-i. Nagaoka, H. Uno, K. Mukai, Kinetic study of the mechanism of free-radical scavenging action in curcumin: effects of solvent and pH, Bull. Chem. Soc. Jpn. 78 (2005) 615–621.
[43] K.Y. Yang, L.C. Lin, T.Y. Tseng, S.C. Wang, T.H. Tsai, Oral bioavailability of curcumin in rat and the herbal analysis from *Curcuma longa* by LC-MS/MS, J. Chromatogr. B, Anal. Technol. Biomed. Life Sci. 853 (2007) 183–189.
[44] D.L. Rymer, T.A. Good, The role of G protein activation in the toxicity of amyloidogenic Abeta-(1-40), Abeta-(25-35), and bovine calcitonin, J. Biol. Chem. 276 (2001) 2523–2530.

[45] D.M. Walsh, A. Lomakin, G.B. Benedek, M.M. Condron, D.B. Teplow, Amyloid beta-protein fibrillogenesis. Detection of a protofibrillar intermediate, J. Biol. Chem. 272 (1997) 22364–22372.
[46] R.V. Ward, K.H. Jennings, R. Jepras, W. Neville, D.E. Owen, J. Hawkins, G. Christie, J. B. Davis, A. George, E.H. Karran, D.R. Howlett, Fractionation and characterization of oligomeric, protofibrillar and fibrillar forms of beta-amyloid peptide, Biochem. J. 348 (Pt 1) (2000) 137–144.
[47] A. Lorenzo, B.A. Yankner, Beta-amyloid neurotoxicity requires fibril formation and is inhibited by congo red, Proc. Natl. Acad. Sci. U. S. A. 91 (1994) 12243–12247.
[48] S.J. Pollack, I.I.J. Sadler, S.R. Hawtin, V.J. Tailor, M.S. Shearman, Sulfated glycosaminoglycans and dyes attenuate the neurotoxic effects of beta-amyloid in rat PC12 cells, Neurosci. Lett. 184 (1995) 113–116.
[49] I.I.J. Sadler, D.W. Smith, M.S. Shearman, C.I. Ragan, V.J. Tailor, S.J. Pollack, Sulphated compounds attenuate beta-amyloid toxicity by inhibiting its association with cells, NeuroReport 7 (1995) 49–53.
[50] W.E. Klunk, M.L. Debnath, A.M. Koros, J.W. Pettegrew, Chrysamine-G, a lipophilic analogue of Congo red, inhibits A beta-induced toxicity in PC12 cells, Life Sci. 63 (1998) 1807–1814.
[51] D.R. Howlett, A.E. Perry, F. Godfrey, J.E. Swatton, K.H. Jennings, C. Spitzfaden, H. Wadsworth, S.J. Wood, R.E. Markwell, Inhibition of fibril formation in beta-amyloid peptide by a novel series of benzofurans, Biochem. J. 340 (1999) 283–289.
[52] T. Tomiyama, H. Kaneko, K. Kataoka, S. Asano, N. Endo, Rifampicin inhibits the toxicity of pre-aggregated amyloid peptides by binding to peptide fibrils and preventing amyloid–cell interaction, Biochem. J. 322 (Pt 3) (1997) 859–865.
[53] T. Tomiyama, A. Shoji, K. Kataoka, Y. Suwa, S. Asano, H. Kaneko, N. Endo, Inhibition of amyloid beta protein aggregation and neurotoxicity by rifampicin. Its possible function as a hydroxyl radical scavenger, J. Biol. Chem. 271 (1996) 6839–6844.
[54] A. Lomakin, D.S. Chung, G.B. Benedek, D.A. Kirschner, D.B. Teplow, On the nucleation and growth of amyloid beta-protein fibrils: detection of nuclei and quantitation of rate constants, Proc. Natl. Acad. Sci. U. S. A. 93 (1996) 1125–1129.
[55] S.J. Wood, L. MacKenzie, B. Maleeff, M.R. Hurle, R. Wetzel, Selective inhibition of Abeta fibril formation, J. Biol. Chem. 271 (1996) 4086–4092.
[56] K. Ono, Y. Yoshiike, A. Takashima, K. Hasegawa, H. Naiki, M. Yamada, Potent anti-amyloidogenic and fibril-destabilizing effects of polyphenols in vitro: implications for the prevention and therapeutics of Alzheimer's disease, J. Neurochem. 87 (2003) 172–181.
[57] F.G. De Felice, M.N. Vieira, L.M. Saraiva, J.D. Figueroa-Villar, J. Garcia-Abreu, R. Liu, L. Chang, W.L. Klein, S.T. Ferreira, Targeting the neurotoxic species in Alzheimer's disease: inhibitors of Abeta oligomerization, Faseb J. 18 (2004) 1366–1372.
[58] R. Liu, H. Barkhordarian, S. Emadi, C.B. Park, M.R. Sierks, Trehalose differentially inhibits aggregation and neurotoxicity of beta-amyloid 40 and 42, Neurobiol. Dis. 20 (2005) 74–81.
[59] M.M. Pallitto, J. Ghanta, P. Heinzelman, L.L. Kiessling, R.M. Murphy, Recognition sequence design for peptidyl modulators of beta-amyloid aggregation and toxicity, Biochemistry 38 (1999) 3570–3578.
[60] C. Soto, E.M. Sigurdsson, L. Morelli, R.A. Kumar, E.M. Castano, B. Frangione, Beta-sheet breaker peptides inhibit fibrillogenesis in a rat brain model of amyloidosis: implications for Alzheimer's therapy, Nat. Med. 4 (1998) 822–826.
[61] C. Hetenyi, Z. Szabo, E. Klement, Z. Datki, T. Kortvelyesi, M. Zarandi, B. Penke, Pentapeptide amides interfere with the aggregation of beta-amyloid peptide of Alzheimer's disease, Biochem. Biophys. Res. Commun. 292 (2002) 931–936.
[62] S. Lee, K. Carson, A. Rice-Ficht, T. Good, Hsp20, a novel {alpha}-crystallin, prevents A{beta} fibril formation and toxicity, Protein Sci. 14 (2005) 593–601.
[63] P. Santhoshkumar, K.K. Sharma, Inhibition of amyloid fibrillogenesis and toxicity by a peptide chaperone, Mol. Cell. Biochem. 267 (2004) 147–155.
[64] B.L. Zhao, X.J. Li, R.G. He, S.J. Cheng, W.J. Xin, Scavenging effect of extracts of green tea and natural antioxidants on active oxygen radicals, Cell Biophys. 14 (1989) 175–185.
[65] S. Martin-Aragon, J.M. Benedi, A.M. Villar, Modifications on antioxidant capacity and lipid peroxidation in mice under fraxetin treatment, J. Pharm. Pharmacol. 49 (1997) 49–52.
[66] L.M. Antunes, M.C. Araujo, J.D. Darin, M.L. Bianchi, Effects of the antioxidants curcumin and vitamin C on cisplatin-induced clastogenesis in Wistar rat bone marrow cells, Mutat. Res. 465 (2000) 131–137.
[67] S.K. Biswas, D. McClure, L.A. Jimenez, I.L. Megson, I. Rahman, Curcumin induces glutathione biosynthesis and inhibits NF-kappaB activation and interleukin-8 release in alveolar epithelial cells: mechanism of free radical scavenging activity, Antioxid. Redox Signal. 7 (2005) 32–41.
[68] A. Rajeswari, Curcumin protects mouse brain from oxidative stress caused by 1-methyl-4-phenyl-1,2,3,6-tetrahydropyridine, Eur. Rev. Med. Pharmacol. Sci. 10 (2006) 157–161.
[69] N. Sreejayan, M.N. Rao, Free radical scavenging activity of curcuminoids, Arzneimittelforschung 46 (1996) 169–171.
[70] B.B. Aggarwal, A. Kumar, A.C. Bharti, Anticancer potential of curcumin: preclinical and clinical studies, Anticancer Res. 23 (2003) 363–398.
[71] J.J. Johnson, H. Mukhtar, Curcumin for chemoprevention of colon cancer, Cancer Lett. 255 (2007) 170–181.
[72] S. Shishodia, M.M. Chaturvedi, B.B. Aggarwal, Role of curcumin in cancer therapy, Curr. Probl. Cancer 31 (2007) 243–305.
[73] B.H. Ali, H. Marrif, S.A. Noureldayem, A.O. Bakheit, G. Blunden, Some biological properties of curcumin: a review, Nat. Prod. Commun. 1 (2006) 509–521.
[74] C. Ramassamy, Emerging role of polyphenolic compounds in the treatment of neurodegenerative diseases: a review of their intracellular targets, Eur. J. Pharmacol. 545 (2006) 51–64.
[75] A.C. Bharti, N. Donato, S. Singh, B.B. Aggarwal, Curcumin (diferuloylmethane) down-regulates the constitutive activation of nuclear factor-kappa B and IkappaBalpha kinase in human multiple myeloma cells, leading to suppression of proliferation and induction of apoptosis, Blood 101 (2003) 1053–1062.
[76] S. Pal, T. Choudhuri, S. Chattopadhyay, A. Bhattacharya, G.K. Datta, T. Das, G. Sa, Mechanisms of curcumin-induced apoptosis of Ehrlich's ascites carcinoma cells, Biochem. Biophys. Res. Commun. 288 (2001) 658–665.
[77] J.H. Woo, Y.H. Kim, Y.J. Choi, D.G. Kim, K.S. Lee, J.H. Bae, D.S. Min, J.S. Chang, Y.J. Jeong, Y.H. Lee, J.W. Park, T.K. Kwon, Molecular mechanisms of curcumin-induced cytotoxicity: induction of apoptosis through generation of reactive oxygen species, down-regulation of Bcl-XL and IAP, the release of cytochrome c and inhibition of Akt, Carcinogenesis 24 (2003) 1199–1208.
[78] G.P. Lim, T. Chu, F. Yang, W. Beech, S.A. Frautschy, G.M. Cole, The curry spice curcumin reduces oxidative damage and amyloid pathology in an Alzheimer transgenic mouse, J. Neurosci. 21 (2001) 8370–8377.
[79] T. Masuda, K. Hidaka, A. Shinohara, T. Maekawa, Y. Takeda, H. Yamaguchi, Chemical studies on antioxidant mechanism of curcuminoid: analysis of radical reaction products from curcumin, J. Agric. Food Chem. 47 (1999) 71–77.
[80] T. Masuda, Y. Toi, H. Bando, T. Maekawa, Y. Takeda, H. Yamaguchi, Structural identification of new curcumin dimers and their contribution to the antioxidant mechanism of curcumin, J. Agric. Food Chem. 50 (2002) 2524–2530.
[81] W. Shi, S. Dolai, S. Rizk, A. Hussain, H. Tariq, S. Averick, W. L'Amoreaux, A. El Ldrissi, P. Banerjee, K. Raja, Synthesis of monofunctional curcumin derivatives, clicked curcumin dimer, and a PAMAM dendrimer curcumin conjugate for therapeutic applications, Org. Lett. 9 (2007) 5461–5464.
[82] L. Breydo, O.V. Bocharova, I.V. Baskakov, Semiautomated cell-free conversion of prion protein: applications for high-throughput screening of potential antiprion drugs, Anal. Biochem. 339 (2005) 165–173.
[83] B. Caughey, L.D. Raymond, G.J. Raymond, L. Maxson, J. Silveira, G.S. Baron, Inhibition of protease-resistant prion protein accumulation in vitro by curcumin, J. Virol. 77 (2003) 5499–5502.
[84] I. Hafner-Bratkovic, J. Gaspersic, L.M. Smid, M. Bresjanac, R. Jerala, Curcumin binds to the alpha-helical intermediate and to the amyloid form of prion protein — a new mechanism for the inhibition of PrP(Sc) accumulation, J. Neurochem. 104 (2008) 1553–1564.
[85] E. Gazit, A possible role for pi-stacking in the self-assembly of amyloid fibrils, Faseb J. 16 (2002) 77–83.
[86] G.G. Tartaglia, A. Cavalli, R. Pellarin, A. Caflisch, The role of aromaticity, exposed surface, and dipole moment in determining protein aggregation rates, Protein Sci. 13 (2004) 1939–1941.